

Study on a-plane GaN etching residual stress using Raman scattering

WANG DANG-HUI^{a,b*}, HAO YUE^a, ZHANG JIN-CHENG^a, XU SHENG-RUI^a, BI ZHI-WEI^a, ZHAO SHENG-LEI^a, MENG FAN-NA^a, XUE XIAO-YONG^a, ZHANG LIN-XIA^a

^a State Key Lab. of Fundamental Science on Wide Band-Gap Semiconductor Technology School of Microelectronics, Xidian University, Xi'an 710071, China

^b School of Materials Science and Engineering of Xi'an ShiYou University, Xi'an 710065, China

In this study, we have studied the etching residual stress for a-plane GaN films grown on r-plane ($\bar{1}102$) sapphire substrate with three different structures by low-pressure metal-organic vapor deposition (LPMOCVD). Scanning electron microscopy (SEM) and Raman scattering have been employed to study the surface morphology and residual stress before and after KOH solution etching. The three phonon modes of E_2 (high), A_1 (TO) and E_1 (TO) and surface etching morphology of a-plane GaN have been observed. We calculated the residual stress using the biaxial elastic stress theory. Conclusions show that E_2 (high) phonon shifts decrease after etching with KOH solution for a-plane GaN epilayer, which shows that KOH solution etching make the residual stress release. Based on the results, we indicated that there exists an approximate linear relation between residual stress etched by KOH solution and biaxial elastic stress system in a-plane GaN epilayers.

(Received March 14, 2012; accepted July 19, 2012)

Keywords: Residual stress, Metal organic chemical vapor deposition, Raman frequency shift, KOH solution etching

1. Introduction

In recent years, the III-Nitride materials and optoelectronic devices have achieved remarkable progress for applications in light-emitting devices (LEDs) covering the ultraviolet and full visible ranges of the electromagnetic spectrum [1]. GaN-based LEDs have experienced considerable success in solid-state lighting. In these structures, spontaneous and piezoelectric induced the electrostatic fields spatially separate the electrons and holes within the quantum wells (QWs), and thereby reduced the irradiative efficiency and making the emission wavelength redshift [2,3,4]. One approach to mitigate these problems is the growth of structures on nonpolar/semipolar orientations substrates [5], for example, a-plane GaN films have been deposited on r-plane sapphire substrate with no polarization fields along the grown orientation. Although nonpolar a-plane GaN structures in r-plane sapphire substrates are preferable in large-scale production, there existed many of questions to be solved, for example, there is very limited supply of semipolar GaN bulk substrates because of their high cost, small area, and complex production procession, and there existed larger strain/stress during the nonpolar GaN structures. Until to today, there are several study teams and many studies on the residual stress of III-V group GaN-based materials by chemical etching have been reported [6-9]. Although many research studies have been carried out on this topic and several papers on this aspect have been published, there have been few general etching residual stress studies of a-plane GaN film after KOH

solution using Raman scattering. Micro-Raman scattering is a fast and nondestructive technique to characterize stress states in III-V group nitrides. In this study, the released GaN etching stress was characterized in micro-Raman backscattering geometry at room temperature, we utilize two times (before KOH solution etching and after KOH solution etching) Raman scattering to study the residual stress of a-plane GaN epilayer in order to avoid the influence that between sapphire substrate and a-plane GaN epilayer, and indicated that there exists an approximate linear relation between the KOH solution etching residual stress and biaxial elastic stress system existed in a-plane GaN epilayers.

2. Experimental procedure

Three different structure a-plane GaN samples were grown on r-plane ($\bar{1}102$) sapphire substrates by metal-organic vapor deposition (MOCVD) system. Three samples with different buffer structures were grown. (A) a LT-AlN of about 30-nm thick, denoted as sample A; (B) a two step (LT and HT) AlN of about 60-nm thick, denoted as sample B; (C) a two step AlN layer and AlN/AlGaIn superlattice (SL) denoted as sample C. Further details about the growth conditions, structure, and properties of nonpolar a-plane GaN grown have been published previously [10,11]. The etching experiments were carried out in 10% (weight fraction) KOH solution in room temperature, after wet chemical etching, we rinse the a-plane GaN film surface with HCl solution and

de-ionized water. Surface morphology was observed by Scanning electron microscopy (SEM) before and after KOH solution etching. Raman scattering were also measured before and after KOH solution etching. The micro-Raman measurements were carried out in backscattering geometry with the Raman spectrometer Jobin Yvon LavRam HR800. An Ar⁺ laser with 514-nm wavelength was used as an excitation light source and a 50 objective was used to focus the incident laser light of a power of 14.2 mW on the samples. The spectrometer was calibrated using single-crystal silicon as a reference. A curve-fitting program was used to fit the Raman spectra to determine the Raman frequencies and linewidths. The program allows peak to be fitted by using a combination of Lorentzian and Gauss peak profiles and subtracting a background.

3. Results and discussions

3.1 Surface etching pits morphology on a-plane GaN epilayers

Fig. 1 shows the typical SEM surface morphology of sample A. Fig. 1 (a) shows that there exist some triangle pits on a-plane GaN epilayer surface. The origin of the pits is not yet clarified, Wu et al. [12] suggested that the pits are pyramidal V-defects, which are distinguished from the V-shaped defects from in *c*-plane GaN by the fact that they are not caused by screw dislocations [13]. Fig. 1 (b) shows that there are much more etch-pits on a-plane epilayer surface through KOH solution etching, which are distinguished from the shape before KOH solution etching. We observed that there are more triangle pits and little pentagonal pits on a-plane epilayer surface before KOH solution etching, these pits are smaller in size and shallower in depth. After KOH solution etching, we found that there are more pentagonal pits on a-plane GaN epilayer surface, and these etch-pits are obviously larger in size and depth. Although there is a tiny change of pit density on sample surface, in fact, the size and depth of etch-pits become larger than before etching due to KOH solution etching. It is KOH solution etching that makes the residual stress between sapphire substrate, buffer layer and epilayer film can be released. One of possible etching mechanism of KOH solution etching is shown in Fig. 2. Neighboring two triangle pits were etched by KOH solution for the reason of large in size and incorporated one pentagonal pit.

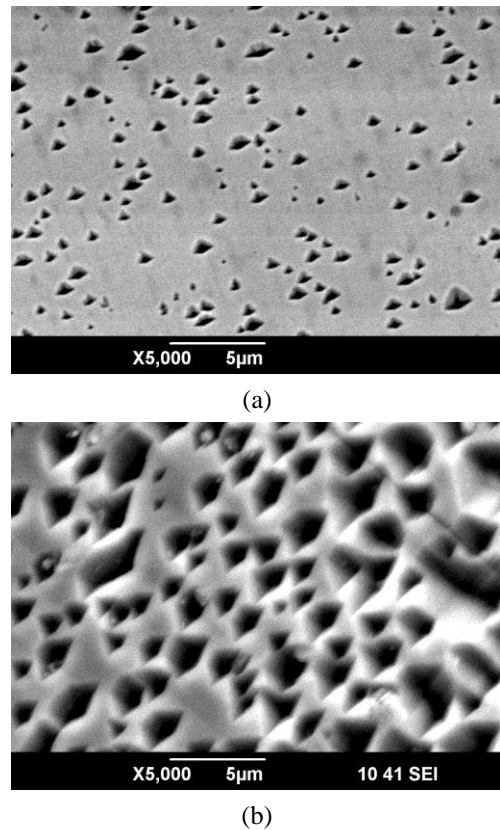


Fig. 1. SEM morphology of surface pits in sample A. (a) before etching; (b) after etching.

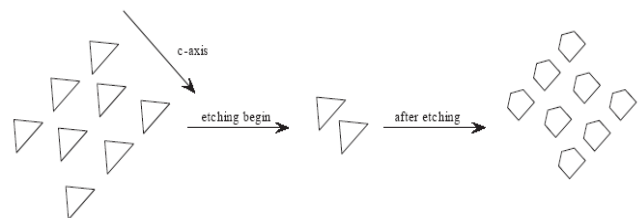


Fig. 2. KOH solution etching mechanism for sample (a).

3.2 Raman scattering in a-plane GaN epilayers

Raman scattering is a standard technique to characterize the strain conditions in III-V alloy systems [14]. Raman scattering were carried out for the three *a*-plane samples before and after the KOH etching solution at room temperature. In order to make the experimental data creditable and comparable, we measured the same point on the surface of the three samples before and after the etching KOH solution. The Raman shifts of the three phonon modes of E₂ (high), A₁ (TO) and E₁ (TO) were measured. Many studies thought that the Raman shift of the GaN E₂ (high) phonon mode is related not only the quality of the crystal, but also residual stress existed in the epilayers [6]. The frequency of E₂ (high) mode is sensitive

to strain as expected from the atomic displacement scheme (of N atoms and perpendicular to the c -axis). A_S can be seen in Fig. 3, under the backscattering $x(yy)\bar{x}$ mode, the E_2 (high) phonon peak appears at 569.50 cm^{-1} before KOH solution etching for sample A, while E_2 (high) phonon peak appears at 568.15 cm^{-1} after KOH solution etching, which is smaller than before KOH solution. Obviously. The similar tendency is also exhibited in sample B and sample C. The reason for change of E_2 (high) phonon peak is that KOH solution makes the residual stress release in a -plane GaN epilayer, and this change can be character by Raman frequency shift of E_2 (high). The relation between the etching residual stress σ and the measured Raman shift of the E_2 (high) phonon line $\Delta\omega$ is derived from the following equation: $\sigma = \Delta\omega/k$. Where σ is in-plane residual stress, and k is the linear stress-shift coefficient ($k=2.40\text{ cm}^{-1}/\text{GPa}$) [15] for the biaxial stress system. The relation shows that the residual compressive stress with 0.5629 GPa , 0.4304 GPa and 0.1896 GPa is induced in a -plane GaN crystal for sample A, B and C, respectively. We listed Raman frequency shifts in Table 1 as following. In fact, we calculate the residual stress of the three samples without using the E_2 (high) phonon peak value $567.5 \pm 0.2\text{ cm}^{-1}$ [16]. In other words, through two times (before and after KOH solution etching)

Raman scattering, we avoid the influence that came from sapphire substrate, and thus improve the residual stress precision for a -plane GaN epilayer.

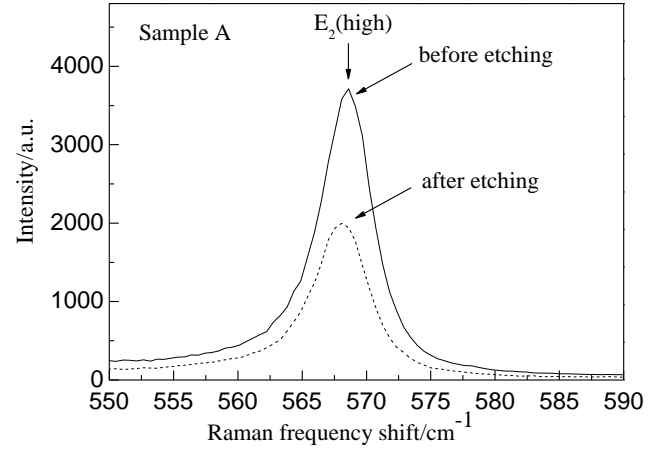


Fig. 3. Raman frequency shifts of sample (a), geometry mode: $x(yy)\bar{x}$.

Table 1. Raman frequency shifts of three samples and their scattering geometry modes.

Backscattering configuration	Active mode	Sample A $\Delta\omega/\text{cm}^{-1}$	Sample B $\Delta\omega/\text{cm}^{-1}$	Sample C $\Delta\omega/\text{cm}^{-1}$
$x(yy)\bar{x}$	$A_1(\text{TO})$	0.00	-0.531	-1.419
	$E_2(\text{High})$	-1.351	-1.033	-0.455
$x(yz)\bar{x}$	$E_1(\text{TO})$	0.00	0.00	-0.504
	$E_2(\text{High})$	-0.086	-1.351	-0.455
$x(zz)\bar{x}$	$A_1(\text{TO})$	-0.530	-0.532	-0.383

Considering the X-axis along $[1\bar{1}20]$, Y-axis along $[1100]$ and Z-axis along $[0001]$ direction, the strain-stress relation for hexagonal crystals with a C_{6v} symmetry matrix can be expressed as [17]:

$$\begin{pmatrix} \sigma_{xx} \\ \sigma_{yy} \\ \sigma_{zz} \end{pmatrix} = \begin{pmatrix} C_{11} & C_{12} & C_{13} \\ C_{12} & C_{11} & C_{13} \\ C_{13} & C_{13} & C_{33} \end{pmatrix} \begin{pmatrix} \varepsilon_{xx} \\ \varepsilon_{yy} \\ \varepsilon_{zz} \end{pmatrix} \quad (1)$$

where C_{ij} are the stiffness constants of a -plane GaN film.

For a -plane nitride epilayers, in the case of a biaxial stress, a lattice constant is fixed, whereas the c lattice constant is free to relax. The biaxial strain is $\varepsilon_{xx} = \frac{a-a_0}{a_0}$, and the strain in the perpendicular direction is given by

$$\varepsilon_{zz} = -\frac{C_{11}}{C_{13}}\varepsilon_{xx} - \frac{C_{12}}{C_{13}}\varepsilon_{yy} \quad (2)$$

We can calculate the residual stress from the equation (2), all of the lattice parameters of a -plane GaN films can be found in Reference [11] in Table 2 and Some mechanical properties of wurtzite GaN listed in Table 2.

Table 2. Lattice constant for samples A, B and C.

Samples	lattice $a(\text{\AA})$
A	3.1945
B	3.1937
C	3.1901

Table 3. Several set of mechanical properties of wurtzite GaN, the units are in GPa.

Parameters	Values
$C_{11}, C_{12}, C_{13}, C_{33}, C_{44}$	377, 160, 114, 209, 81.4 [18]
$C_{11}, C_{12}, C_{13}, C_{33}, C_{44}$	390, 145, 106, 398, 105 [19]
Poisson's ratio	0.372 [20], 0.38

Using equation (2) and Table 3, we can obtain the stress value of 0.7275GPa, 0.6082GPa and 0.1424GPa for sample (a), (b) and (c), respectively.

In order to probe the dependence of the two methods for calculating residual stress, we plot the function relation between change of Raman frequency shifts and biaxial elastic stress for *a*-plane GaN epilayer, as shown in Fig. 4. We can find that there exists an approximate linear relation between biaxial elastic stress and residual stress calculated by change of Raman frequency shifts for *a*-plane GaN epilayer. From discussion above, the conclusion can be obtained that the two methods that character the residual stress for *a*-plane GaN epilayer exists a simple linear relation. One of the disadvantages of the method is that the KOH solution etching can avoid the influence of sapphire substrate and improve the precision of the residual stress. And so we can characterize and calculate the etching residual stress by Raman scattering.

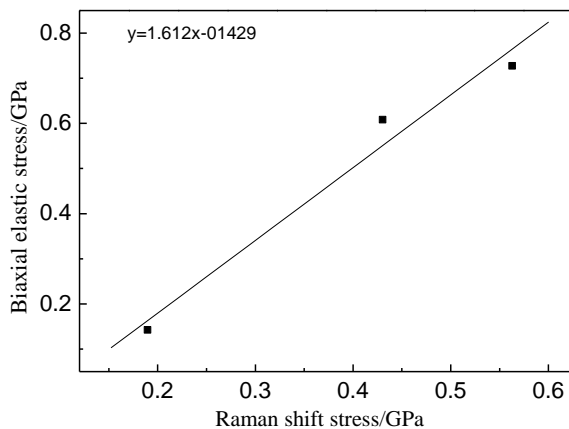


Fig. 4. Relation between biaxial elastic stress and calculated stress by Raman frequency shifts.

4. Conclusions

In summary, we present a micro-Raman scattering study on *a*-plane GaN epilayer residual stress by KOH etching solution. After KOH solution etching, E_2 (high) frequency shifts changes to lower frequency shifts compared with before KOH solution etching, which shows that etching make the residual stress release. And a simple approximate linear relation exists between the two methods to calculate residual stress, which indicates that Raman scattering frequency shifts can be used to characteristic the residual stress of KOH solution etching

for semiconductor materials.

Acknowledgements

This work was supported by the National Key Science & Technology Special Project (Grant No. 2008ZX01002-002), the Fundamental Research Funds for the Central Universities (Grant No. JY10000904009), the Major Program and State Key Program of National Natural Science Foundation of China (Grant No. 60890191 and 60736033).

References

- [1] S. R. Xu et al., Jpn. J. Appl. Phys. **50**, 115502 (2011).
- [2] C. Netzela, T. Wernicke, U. Zeimer, et al., J. Cryst. Growth. **310**, 8 (2008).
- [3] Kazuhide Kusakabe, Shizutoshi Ando, Kazuhiro Ohkaw, J. Cryst Growth **298**, 293 (2007).
- [4] M. Kuroda, H. Ishida, J. Appl. Phys. **102**, 093703 (2007).
- [5] P. Waltereit, O. Brandt, A. Trampert, et al., Nature **406**, 865 (2000).
- [6] S. Tripathy, Vivian K. X. Lin, S. Vicknesh, et al., J. Appl. Phys. **101**, 063525 (2007).
- [7] Y. Gao, M. D. Craven, J. S. Speck, et al., Applied Physics Letters, **84**, 3322 (2004).
- [8] M. Lu et al., **45**, December, 673 (2004).
- [9] D. C. Hays, C. R. Abernathy, S. J. Pearton, R. J. Shul, G. A. Vawter, J. Han in IEEE Journal of Selected Topics in Quantum Electronics (1998).
- [10] S. R. Xu, J. C. Zhang, Z. M. Li, et al., Acta Physica Sinica. **8**, 5705 (2009).
- [11] S. R. Xu, Y. Hao, J. C. Zhang, et al., J. Cryst. Growth **311**, 3622 (2009).
- [12] F. Wu, M. D. Craven, S. H. Lim, et al., J. Applied Physics, **94**, 942 (2003).
- [13] A. N. Bright, N. Sharma, C. J. Humphreys, Journal of Electron Microscopy, **50**, 489 (2001).
- [14] S. Hernández, N. Blanco, I. Mártil, et al., J. Appl. Phys. **93**, 9019 (2003).
- [15] J. W. Ager III, G. Conti, L. T. Romano, C. Kisielowski, MRS Symp. Proc. **482**, 769 (1998).
- [16] G. Irmer, T. Brumme, M. Herms, et al., J. Mater. Sci: Mater Electron **19**, 51 (2008).
- [17] Group III Nitride semiconductor compound-Physics and Applications. Bernard Gil. Clarendon Press-Oxford page 316.
- [18] R. B. Schwarz, K. Khachataryan, E. R. Weber: Appl. Phys. Lett. **70**, 1122 (1997).
- [19] A. Polian, M. Grimsditch, I. Grzegory: J. Appl. Phys. **79**, 3343 (1996).
- [20] T. Detchprohm, K. Hiramatsu, K. Itoh, I. Akasaki: Jpn. J. Appl. Phys. **31**, L1454 (1992).

*Corresponding author: wdhyxp@163.com